Published online 22 December 2010

Nucleic Acids Research, 2011, Vol. 39, No. 6 ***e37***
doi:10.1093/nar/gkq1294

Conjugation polymer nanobelts: a novel fluorescent sensing platform for nucleic acid detection†

Lei Wang[1], Yingwei Zhang[1], Jingqi Tian[1,2], Hailong Li[1,2] and Xuping Sun[1,*]

[1]State Key Laboratory of Electroanalytical Chemistry, Changchun Institute of Applied Chemistry, Chinese Academy of Sciences, Changchun 130022, Jilin and [2]Graduate School of the Chinese Academy of Sciences, Beijing 100039, People's Republic of China

Received August 16, 2010; Revised November 12, 2010; Accepted December 3, 2010

ABSTRACT

In this article, we report on the facile and rapid synthesis of conjugation polymer poly(*p*-phenylenediamine) nanobelts (PNs) via room temperature chemical oxidation polymerization of *p*-phenylenediamine monomers by ammonium persulfate in aqueous medium. We further demonstrate the proof-of-concept that PNs can be used as an effective fluorescent sensing platform for nucleic acid detection for the first time. The general concept used in this approach lies in the facts that the adsorption of the fluorescently labeled single-stranded DNA probe by PN leads to substantial fluorescence quenching, followed by specific hybridization with the complementary region of the target DNA sequence. This results in desorption of the hybridized complex from PN surface and subsequent recovery of fluorescence. We also show that the sensing platform described herein can be used for multiplexing detection of nucleic acid sequences.

INTRODUCTION

The past years have witnessed the growing interest in nucleic acid-based diagnostic tests. The intensive development of systems allowing rapid, cost-effective sensitive and specific detection of nucleic acid is motivated by their various applications in many fields such as, gene analysis, clinical disease diagnostics and treatment, fast detection of biological warfare agents and forensic applications, etc. (1). The humanitarian and economic costs of infectious diseases can be greatly reduced by accurate diagnosis that enables prompt treatment. Detecting genetic mutations at the molecular level opens up the possibility of performing reliable disease diagnostics in clinical practice even before any symptom of a disease appears. Until now, numerous optical and electrochemical nucleic acid detection approaches based on the hybridization between a target and its complementary probe have been successfully established (2). The introduction of simple methods for fluorescent labeling of nucleic acids has opened the door that enables nucleic acid hybridization probes to be used for research and development, and indeed, in recent years, fluorescent probes have multiplied at a high rate and the homogeneous fluorescence assays based on fluorescence resonance energy transfer (FRET) or quenching mechanism for nucleic acid detection have been widely developed (3). Among such probes, Taqman probes, molecular beacons (MBs) and Scorpions are labeled with both a fluorescent reporter and a quencher dye and the fluorescence is only released from the reporter when the two dyes are physically separated after hybridization occurs. Although widely used for many applications (3–7), they require labeling at both ends with specific dyes that suffer from low overall yield and are not cost-effective (8). To solve these problems, single fluorophore-labeled probe with only one fluorophore tag has been developed; however, guanine bases (8) or nanostructures (9) must be used as a 'nanoquencher' at the same time to effectively signal target detection event. It has been demonstrated that nanostructures can also be used as a nanoquencher of the fluorophore (9,10). Because the same nanostructure has the ability to quench dyes of different emission frequencies, the selection issue of a fluorophore–quencher pair is eliminated from the nanostructure-based system. In principal, nanostructures suitable as an ideal platform for this assay should satisfy the following two requirements: (i) They have strong binding with single-stranded DNA (ssDNA), but weak even when not binding with double-stranded DNA (dsDNA) and (ii) they do not fluoresce or only have weak fluorescence and quench dye fluorescence very effectively at the same time. So far, however, only limited nanostructures, including gold nanoparticles (9,11–13), single-walled carbon nanotubes

*To whom correspondence should be addressed. Tel/Fax: +86 431 85262065; Email: sunxp@ciac.jl.cn

†Dedicated to Prof. Shaojun Dong in honor of her 80th birthday.

(SWCNTs) (10,14) and graphene (15,16) have been demonstrated for such application. Although gold nanoparticle is able to discriminate single-base mismatch, its small size makes it hard for simultaneous adsorption of multiple DNA probes labeled with different dyes on the same particle surface and hence multiplexing nucleic acid detection is difficult to achieve. For the SWCNT or graphene system, it suffers from both SWCNT and graphite powder used for producing graphene are usually purchased from some sources on one hand, and an organic solvent like *N,N*-dimethylformamide (DMF) is used to disperse SWCNT by a period of several hours sonication (14) or the graphene preparation by the Hummer's method is time-consuming and labor intensive (17). Accordingly, it is crucially important to develop new nanostructures that can be used as an effective fluorescent sensing platform for multiplexing nucleic acid detection.

In this article, we report on the facile and rapid synthesis of conjugation polymer poly(*p*-phenylenediamine) (PPPD) nanobelts (PNs) via room temperature chemical oxidation polymerization of *p*-phenylenediamine (PPD) monomers by ammonium persulfate (APS) in aqueous medium. As a proof of concept, we demonstrate for the first time that PNs can be used as an effective fluorescent sensing platform capable of discrimination of complementary and single-base mismatched target sequences. The general concept used in this approach is based on the adsorption of the fluorescently labeled ssDNA probe by PN, which is accompanied by substantial fluorescence quenching, followed by specific hybridization with its target to form dsDNA. This results in desorption of the hybridized complex from PN surface and subsequent recovery of fluorescence. We further demonstrate that the sensing platform described herein can be used for multiplexing detection of nucleic acid sequences.

Scheme 1 presents a schematic diagram to illustrate the fluorescence-enhanced nucleic acid detection using PPPD nanobelt as a sensing platform. The zeta potential of the nanobelt was measured to be about 1.06 mV, meaning that the nanobelt has an overall low positively charged surface. Therefore, the electrostatic attractive interactions between PN and negatively charged backbone of ssDNA contribute little to the binding of ssDNA to PN. PN is a π-rich conjugation polymer and thus ssDNA can adsorb strongly on the PN surface via π–π stacking interactions of DNA bases on PN (18). In contrast, PN should have no binding with dsDNA because there are no π-stacking effects between them in the absence of free nucleobases and nucleosides. The DNA detection is accomplished by two steps: in the first step, the adsorption of fluorescent carboxyfluorescein (FAM)-labeled ssDNA onto the nanobelt leads to substantial fluorescence quenching due to their close approximation. In the second step, the specific hybridization of the dye-labeled DNA with its target leads to fluorescence recovery because such hybridization will disturb the interaction between the dye-labeled ssDNA and nanobelt and produces a dsDNA that detaches from PN.

MATERIALS AND METHODS

All chemically synthesized oligonucleotides were purchased from Shanghai Sangon Biotechnology Co. Ltd (Shanghai, China). DNA concentration was estimated by measuring the absorbance at 260 nm. All the other chemicals were purchased from Aladin Ltd, (Shanghai, China) and used as received without further purification. The water used throughout all experiments was purified through a Millipore system. The PNs were prepared as follows: in brief, 0.9 ml of 0.6 M APS was added into 0.9 ml of 0.2 M PPD aqueous solution at room temperature under shaking. After that, a large amount of precipitates gradually occurred within minutes. The resulting precipitates were washed with water by centrifugation twice first, and then redispersed in water and stored at 4°C for characterization and further used. Oligonucleotide sequences used are listed below (mismatch underlined):

(1) FAM dye-labeled ssDNA (P_{HIV}):
5′-FAM-AGT CAG TGT GGA AAA TCT CTA GC-3′
(2) Complementary target to P_{HIV} (T_1):
5′-GCT AGA GAT TTT CCA CAC TGA CT-3′
(3) Single-base mismatched target to P_{HIV} (T_2): 5′-GCT AGA GAT T<u>G</u>T CCA CAC TGA CT-3′
(4) Non-complementary target to P_{HIV} (T_3):
5′-TTT TTT TTT TTT TTT TTT TTT TT-3′
(5) 5′-TGG AAA ATC-3′ (P_s)
(6) 5′-GAT TTT CCA-3′ (T_{s1})
(7) 5′-GAT T<u>G</u>T CCA-3′ (T_{s2})
(8) 5′-TTT T<u>T</u>T TTT-3′ (T_{s3})
(9) ROX dye-labeled ssDNA (P_{HBV}):
5′-ROX-TAC CAC ATC ATC CAT ATA ACT GA-3′

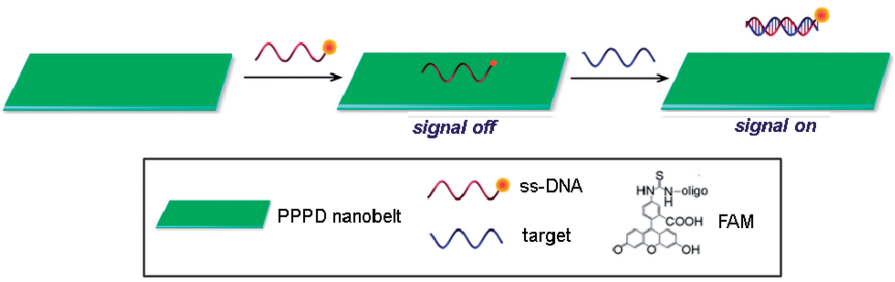

Scheme 1. A schematic diagram (not to scale) to illustrate the fluorescence-enhanced nucleic acid detection using PPPD nanobelt as a sensing platform.

(10) Complementary target to P_{HBV} (T_4):
5′-TCA GTT ATA TGG ATG ATG TGG TA-3′
(11) Cy5 dye-labeled ssDNA (P_{K167}):
5′-Cy5-TCT GCA CAC CTC TTG ACA CTC CG-3′
(12) Complementary target to P_{K167} (T_5):
5′-CGG AGT GTC AAG AGG TGT GCA GA-3′

Scanning electron microscopy (SEM) measurements were made on a XL30 ESEM FEG SEM at an accelerating voltage of 20 kV. Transmission electron microscopy (TEM) measurements were made on a HITACHI H-8100 EM (Hitachi, Tokyo, Japan) with an accelerating voltage of 200 kV. Fluorescent emission spectra were recorded on a PerkinElmer LS55 Luminescence Spectrometer (PerkinElmer Instruments, UK). Zeta potential measurements were performed on a Nano-ZS Zetasizer ZEN3600 Instrument (Malvern Instruments Ltd, UK).

RESULTS AND DISCUSSION

Figure 1 shows typical SEM and TEM images of the products thus formed. Low magnification SEM image shown in Figure 1a indicates that the products exclusively consist of a large quantity of one-dimensional (1D) microstructures about tens of micrometers in length. A high magnification SEM image shown in Figure 1b further reveals that such 1D structure is belt in shape and about several hundred-nanometers in width, which is also evidenced by low magnification TEM image (Figure 1c). A local magnification of a single belt by TEM shows that it has perfectly smooth surface (Figure 1d). Although, we failed to obtain the height information of the belts, their transparent nature provides a clear piece of evidence to support the formation of thin PPPD nanobelts (see Supplementary Figure S1 for chemical analysis of nanobelts).

We test the feasibility of the PN as a fluorescent sensing platform for nucleic acid detection. Figure 2 shows the fluorescence emission spectra (excitation at 480 nm) of P_{HIV} at different conditions. The fluorescence spectrum of P_{HIV}, the FAM-labeled probe, in Tris–HCl buffer in the absence of PN exhibits strong fluorescence emission due to the presence of the fluorescein-based dye (curve a). However, in the presence of 40-μl PN sample (see Supplementary Figure S2 for the optimization details of the ratio between PNs and the oligonucleotide), up to 92% quenching of the fluorescence emission was observed (curve c), indicating strong adsorption of the ssDNA probe on PN and high fluorescence quenching efficiency of PN. On the other hand, the P_{HIV}–PN complex had significant fluorescence enhancement upon its incubation with complementary target T_1 over a period of 1 h, leading to a 55% fluorescence recovery (curve d). It should be noted that the fluorescence of the free P_{HIV} was, however, scarcely influenced by the addition of T_1 in the absence of PN (curve b). We further measured the fluorescence intensity changes (F/F_0-1) of P_{HIV}–PN complex upon addition of different concentrations of T_1 ranging from 30 to 300 nM, where F_0 and F correspond to the fluorescence intensities at 522 nm in the absence and the presence of the target, respectively, and found that a good linear relationship is obtained in the range of 30–300 nM (inset). Also, note that the PN itself shows weak fluorescence emission (curve e), which also contributes to the fluorescence intensity of each sample examined, so a background subtraction is performed for all PN-involved samples measured.

We further studied the kinetic behaviors of P_{HIV} and PN, as well as of the P_{HIV}–PN complex with T_1 by collecting the time-dependent fluorescence emission spectra. Figure 3a shows the fluorescence quenching of P_{HIV} in the presence of PN as a function of incubation time. In the absence of the target, the curve exhibits a rapid reduction in the first 15 min and reaches gradually equilibrium within the following 15 min, indicating that ssDNA adsorption on PN is much faster than on SWCNT (65 min) but slower than on graphene (2 min) (10,15). Figure 3b shows the fluorescence recovery of P_{HIV}–PN by T_1 as a function of time. In the presence of the target T_1, the curve shows a fast increase in the first 10 min, followed by a slow enhancement over a period of 45 min. The best fluorescence response was obtained after about 1 h of incubation time. Therefore, the kinetics of the hybridization of the probe adsorbed on PN to its target and the subsequent release of the dsDNA thus formed from PN is also slower than on graphene (30 min) but faster than on SWCNT (65 min) (10,15). We also investigated the influence of temperature on the kinetic behaviours of these two processes. Supplementary Figure S3 shows the corresponding results obtained at 50°C, indicating that only about 10 min is required to reach equilibrium for both the quenching and the subsequent recovery process. It should be noted that FAM-ssDNA only exhibits slight fluorescence decrease at increased temperature. The observed decrease of FAM fluorescence intensity at elevated temperature in our present study can be attributed to hybridization stringency conditions that do not favour duplex formation between short single strands (19), leading to decreased hybridization and thus fluorescence recovery efficiency.

Figure 4a shows the fluorescence responses of P_{HIV}–PN complex toward complementary target T_1, single-base mismatched target T_2 and non-complementary target T_3. The F/F_0 value obtained upon addition of 300 nM of T_2 is about 91.2% of the value obtained upon addition of 300 nM of T_1 into P_{HIV}–PN complex at room temperature of 25°C (where F_0 and F are the fluorescence intensity without and with the presence of target, respectively). However, only very small fluorescence enhancement was observed for the P_{HIV}–PN upon addition of 300 nM T_3, indicating that the observed fluorescence enhancement in our present system is indeed due to the base pairing between probe and its target. Compared to the complementary target T_1, the mismatched target T_2 should have lower hybridization ability toward the adsorbed dye-labeled ssDNA probe. As a result, a decreased hybridization and thus fluorescence recovery efficiency was expected. Figure 4a inset presents the corresponding fluorescence intensity histograms with error bar, indicating the results obtained exhibits good reproducibility. We also

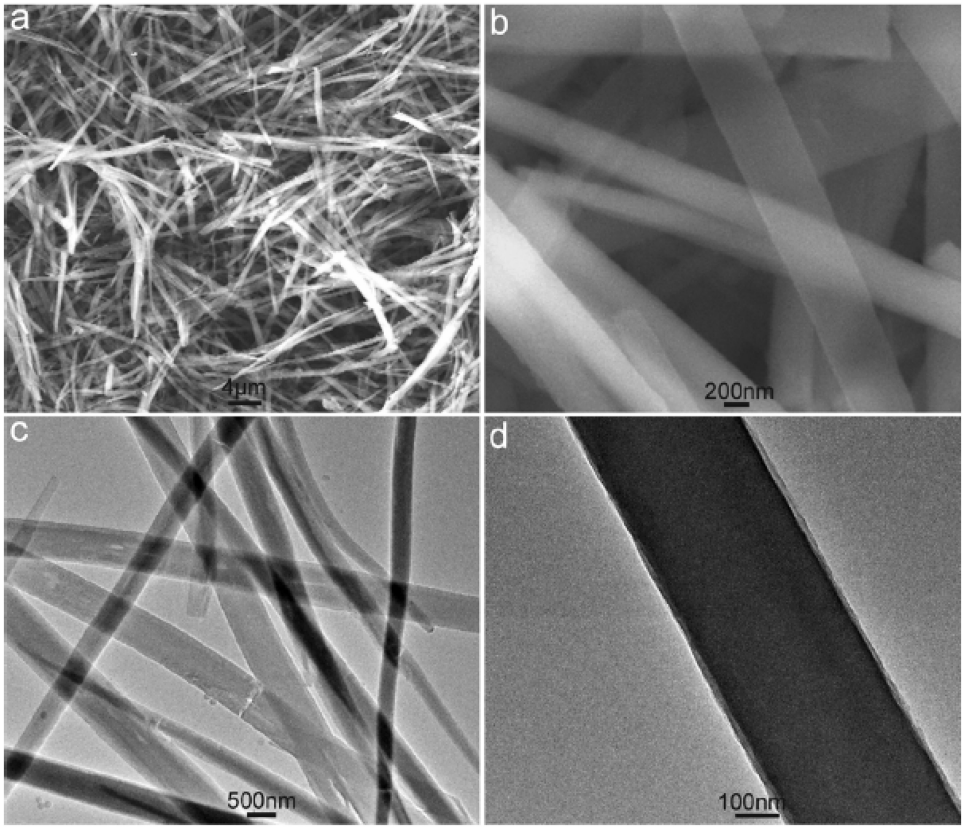

Figure 1. Low magnification SEM (**a**) and TEM (**c**) images of the products thus formed. (**b** and **d**) Indicates the corresponding high magnification images.

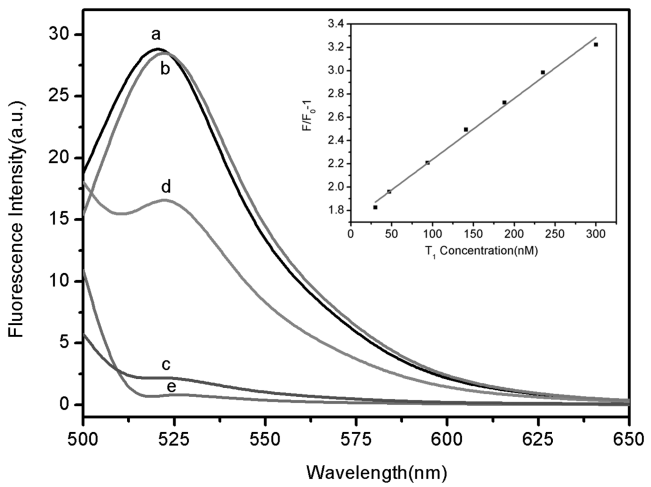

Figure 2. Fluorescence emission spectra of P_{HIV} (50 nM) at different conditions: (a) P_{HIV}; (b) P_{HIV} + 300 nM T_1; (c) P_{HIV} + PN; (d) P_{HIV} + PN + 300 nM T_1. Curve e is the emission spectra of PN. Inset: linear relationship between F/F_0-1 (where F_0 and F are the fluorescence intensity without and with the presence of T_1, respectively) and T_1 concentration ranging from 30 to 300 nm. Excitation was at 480 nm, and the emission was monitored at 522 nm. All measurements were done in Tris–HCl buffer in the presence of 5 mM Mg^{2+} (pH: 7.4).

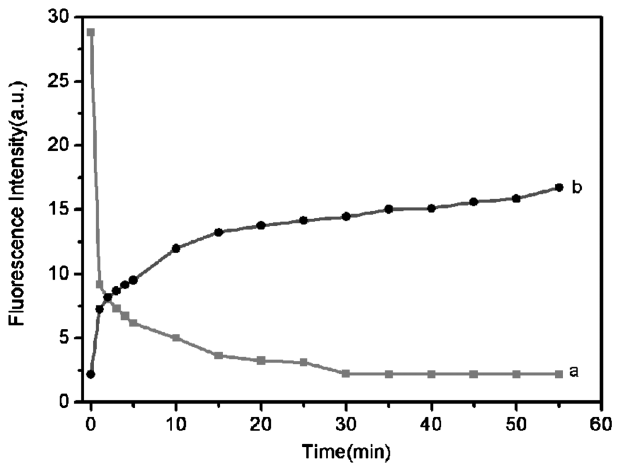

Figure 3. (a) Fluorescence quenching of P_{HIV} (50 nM) by PN and (b) fluorescence recovery of P_{HIV}–PN by T_1 (300 nM) as a function of incubation time. Excitation was at 480 nm, and the emission was monitored at 522 nm. All measurements were done in Tris–HCl buffer in the presence of 5 mM Mg^{2+} (pH: 7.4).

performed hybridization experiments at elevated temperature of 50°C and found that the F/F_0 value obtained upon addition of T_2 is about 81% of the value obtained upon addition of T_1 into P_{HIV}–PN complex. Figure 4b compares the fluorescence signal enhancement of P_{HIV}–PN complex upon incubation with T_1 and T_2 at 25 and 50°C, respectively. All the above observations indicate that the present nucleic acid detection system can distinguish complementary and mismatched nucleic acid sequences and its discriminating ability increases with increased temperature, which makes the hybridization

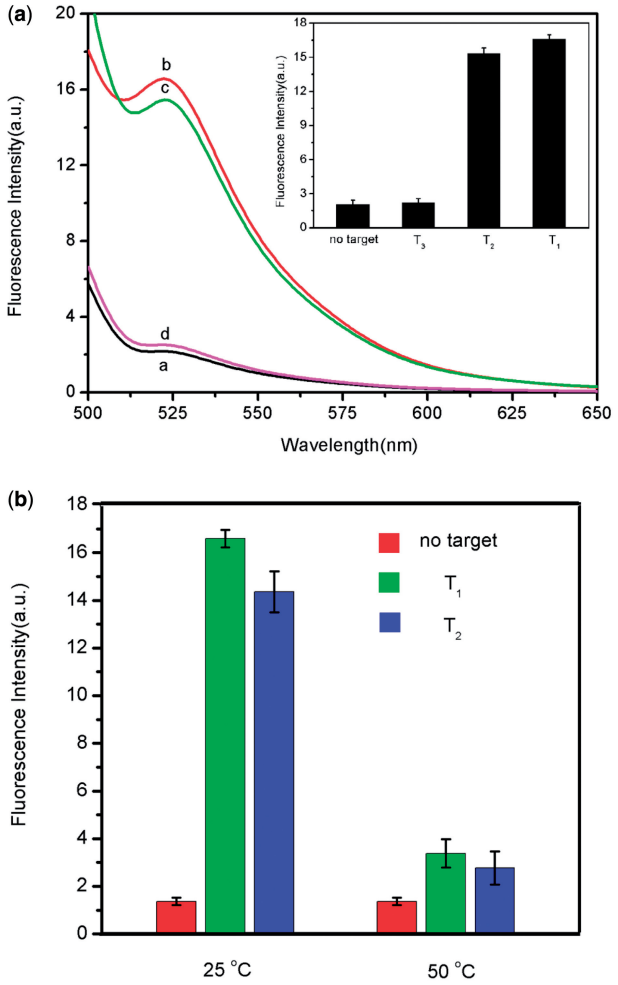

Figure 4. (a) Fluorescence emission spectra of P_{HIV} (50 nM) at different conditions: (a) P_{HIV}–PN complex; (b) P_{HIV}–PN complex + 300 nM T_1; (c) P_{HIV}–PN complex + 300 nM T_2; (d) P_{HIV}–PN complex + 300 nM T_3. Inset: fluorescence intensity histograms with error bar. (**b**) Fluorescence signal enhancement of P_{HIV}–PN complex upon incubation with T_1 and T_2 at 25 and 50°C, respectively. Excitation was at 480 nm, and the emission was monitored at 522 nm. All measurements were done in Tris–HCl buffer in the presence of 5 mM Mg^{2+} (pH: 7.4).

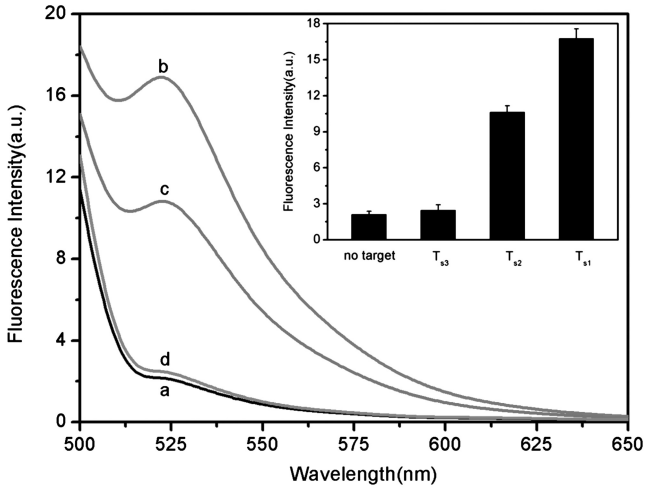

Figure 5. (**a**) Fluorescence emission spectra of P_s (50 nM) at different conditions: (a) P_s–PN complex; (b) P_s–PN complex + 300 nM T_{s1}; (c) P_s–PN complex + 300 nM T_{s2}; (d) P_s–PN complex + 300 nM T_{s3}. Inset: fluorescence intensity histograms with error bar.

harder for probe and mismatched target. It is important to note that the use of shorter oligonucleotide can distinctly improve the mismatch discrimination ability of our present sensing system. Figure 5 shows the fluorescence responses of FAM-labeled, 9-nt ssDNA probe P_s (50 nM) toward complementary target T_{s1}, single-base mismatched target T_{s2} and non-complementary target T_{s3} at room temperature, in the presence of PN. The F/F_0 value obtained upon addition of 300 nM of T_{s2} is about 64.2% of the value obtained upon addition of 300 nM of T_{s1} into P_s–PN complex.

Multiplexing detection of nucleic acid sequences is a challenging task for many assays because of the need of eliminating probe set/target set cross -reactivity, minimizing non-specific binding and designing spectroscopically and chemically unique probes (20), which prompted us to explore the feasibility of using the platform described herein to detect multiple DNA targets simultaneously. To this end, we chose FAM-labelled P_{HIV} and another two probes P_{HBV} and P_{K167} labelled with ROX and Cy5 (cyanine 5), respectively, as model systems. Because these three dyes were individually excited at 480, 587 and 643 nm to emit at 522, 606 and 665 nm, respectively, significant dye-to-dye energy transfer was avoided. In the presence of PN, the fluorescence of all dyes in the probe mixture was heavily quenched, suggesting that PN can effectively quench dyes of different emission frequencies. Figure 6 shows the fluorescence intensity histograms of the probe mixture toward different target combinations in the presence of PN under excitation/emission wavelengths of 480/522, 587/606 and 643/665 nm/nm. It is clearly seen that the addition of T_1 gives only one strong emission peak at 522 nm when excited at 480 nm. However, the target combination of T_1+T_5 gives two strong emission peaks at 522 and 665 nm when excited at 480 and 643 nm, respectively, and three strong emission peaks are observed for the T_1+T_4+T_5 target combination at 522, 606 and 665 nm when excited at 480, 587 and 643 nm, respectively. Based on all the above observations, it can be concluded that this sensing platform can be used for multiplexing detection of nucleic acid sequences.

In conclusion, conjugation polymer PNs were facilely synthesized for the first time via chemical oxidation polymerization method. As a proof of concept, we demonstrate the use of such nanobelts as an effective sensing platform for fluorescence-enhanced nucleic acid detection capable of discrimination of complementary and single-base mismatched target sequences. Furthermore, we show that this approach can be used for multiplexing detection of nucleic acid sequences. Our present observations are significant because it not only provides us a facile method for the synthesis of conjugation polymer nanobelts for nucleic acid detection and other applications, but also will open the door to explore the use of conjugated or π-rich nanostructures as a promising,

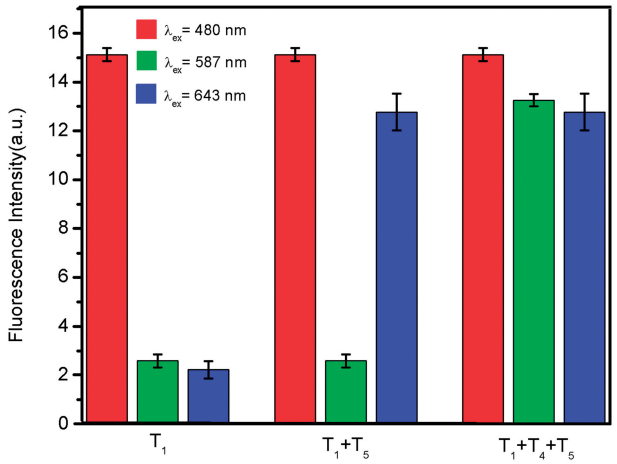

Figure 6. Fluorescence intensity histograms of the probe mixture toward different target combinations in the presence of PN under excitation/emission wavelengths of 480/522, 587/606 and 643/665 nm/nm. All measurements were done in Tris–HCl buffer in the presence of 5 mM Mg^{2+} (pH: 7.4).

universal and effective sensing platform for a fluorescence-enhanced detection sensitive and selective to the target molecule studied.

SUPPLEMENTARY DATA

Supplementary Data are available at NAR Online.

FUNDING

National Basic Research Program of China (No. 2011CB935800). Funding for open access charge: Ministry of Science and Technology of the People's Republic of China.

Conflict of interest statement. None declared.

REFERENCES

1. Gresham,D., Ruderfer,D.M., Pratt,S.C., Schacherer,J., Dunham,M.J., Botstein,D. and Kruglyak,L. (2006) Genome-wide detection of polymorphisms at nucleotide resolution with a single DNA microarray. *Science*, **311**, 1932–1936.
2. Sassolas,A., Leca-Bouvier,B.D. and Blum,L.J. (2008) DNA biosensors and microarrays. *Chem. Rev.*, **108**, 109–139.
3. Didenko,V.V. (ed.), (2006) *Fluorescent Energy Transfer Nucleic Acid Probes: designs and Protocols*. Human Press, Totowa, NJ.
4. Holland,P.M., Abramson,R.D., Watson,R. and Gelfand,D.H. (1991) Detection of specific polymerase chain reaction product by utilizing the 5′→3′ exonuclease activity of Thermus aquaticus DNA polymerase. *Proc. Natl Acad. Sci. USA*, **88**, 7276–7280.
5. Tyagi,S. and Kramer,F.R. (1996) Molecular beacons: probes that fluoresce upon hybridization. *Nat. Biotechnol.*, **14**, 303–308.
6. Yang,C.J., Medley,C.D. and Tan,W. (2005) Monitoring nucleic acids using molecular beacons. *Curr. Pharm. Biotechnol.*, **6**, 445–452.
7. Marras,S.A.E. (2006) Selection of fluorophore and quencher pairs for fluorescent nucleic acid hybridization probes. *Methods Mol. Biol.*, **335**, 3–16.
8. Misra,A.P., Kumar,P. and Gupta,K.C. (2007) Synthesis of hairpin probe using deoxyguanosine as a quencher: Fluorescence and hybridization studies. *Anal. Biochem.*, **364**, 86–88.
9. Ray,P.C., Darbha,G.K., Ray,A., Walker,J. and Hardy,W. (2007) Gold nanoparticle based FRET for DNA detection. *Plasmonics*, **2**, 173–183.
10. Yang,R., Tang,Z., Yan,J., Kang,H., Kim,Y., Zhu,Z. and Tan,W. (2008) Noncovalent assembly of carbon nanotubes and single-stranded DNA: an effective sensing platform for probing biomolecular interactions. *Anal. Chem.*, **80**, 7408–7413.
11. Dubertret,B., Calame,M. and Libchaber,A.J. (2001) Single-mismatch detection using gold-quenched fluorescent oligonucleotides. *Nat. Biotechnol.*, **19**, 365–370.
12. Maxwell,D.J., Taylor,J.R. and Nie,S. (2002) Self-assembled nanoparticle probes for recognition and detection of biomolecules. *J. Am. Chem. Soc.*, **124**, 9606–9612.
13. Li,H. and Rothberg,L.J. (2004) DNA sequence detection using selective fluorescence quenching of tagged oligonucleotide probes by gold nanoparticles. *Anal. Chem.*, **76**, 5414–5417.
14. Yang,R., Jin,J., Chen,Y., Shao,N., Kang,H., Xiao,Z., Tang,Z., Wu,Y., Zhu,Z. and Tan,W. (2008) Carbon nanotube-quenched fluorescent oligonucleotides: probes that fluoresce upon hybridization. *J. Am. Chem. Soc.*, **130**, 8351–8358.
15. Lu,C., Yang,H., Zhu,C., Chen,X. and Chen,G. (2009) A Graphene platform for sensing biomolecules. *Angew. Chem. Int. Ed.*, **48**, 4785–4787.
16. He,S., Song,B., Li,D., Zhu,C., Qi,W., Wen,Y., Wang,L., Song,S., Fang,H. and Fan,C. (2010) A graphene nanoprobe for rapid, sensitive, and multicolor fluorescent DNA analysis. *Adv. Funct. Mater.*, **20**, 453–459.
17. Hummers,W.S. and Offeman,R.E. (1958) Preparation of graphitic oxide. *J. Am. Chem. Soc.*, **80**, 1339.
18. Varghese,N., Mogera,U., Govindaraj,A., Das,A., Maiti,P.K., Sood,A.K. and Rao,C.N.R. (2009) Binding of DNA nucleobases and nucleosides with graphene. *ChemPhysChem*, **10**, 206–210.
19. Burr,H.E. and Schimke,R.T. (1982) Reduced-stringency DNA reassociation: sequence specific duplex formation. *Nucleic Acids Res.*, **10**, 719–733.
20. Stoeva,S.I., Lee,J.-S., Thaxton,C.S. and Mirkin,C.A. (2006) Multiplexed DNA detection with biobarcoded nanoparticle probe. *Angew. Chem. Int. Ed.*, **45**, 3303–3306.